Exact solution for SU(2)-symmetry-breaking bosonic mixtures at strong interactions

Gianni Aupetit-Diallo,[1] Giovanni Pecci,[2] Charlotte Pignol,[1] Frédéric Hébert,[1] Anna Minguzzi,[2] Mathias Albert,[1] and Patrizia Vignolo[1]

[1]*Université Côte d'Azur, CNRS, Institut de Physique de Nice, 06560 Valbonne, France*

[2]*Univ. Grenoble Alpes, CNRS, LPMMC, 38000 Grenoble, France*

(Received 15 June 2022; revised 30 August 2022; accepted 31 August 2022; published 12 September 2022; corrected 23 December 2022 and 13 November 2023)

We study the equilibrium properties of a one-dimensional mixture of two Tonks-Girardeau gases on a ring geometry in the limit of strongly repulsive interspecies interactions. We derive the exact many-body wave function and compare it to the SU(2) solution where intra- and interspecies interactions are also diverging but equal. We focus on the role of the SU(2) symmetry breaking on the behavior of the large- and short-distance correlations by studying the zero-momentum occupation number and the Tan's contact from the asymptotic behavior of the momentum distribution. Although the symmetry is only weakly broken, it has important consequences on spin correlations in the system as the reduction by a factor of two of the zero-momentum occupation number with respect to the SU(2) case in the thermodynamic limit and the decrease of the Tan's contact.

DOI: 10.1103/PhysRevA.106.033312

I. INTRODUCTION

Ultracold atomic mixtures are an important paradigm for quantum simulators due to their extreme versatility. Such systems offer the possibility to control most of the microscopic parameters such as dimensionality, interaction strength and range, the number of spin components, the number of atoms, and external potentials while giving access to many physical observables, including those intimately connected to quantum correlations.

In particular one-dimensional (1D) mixtures are of significant importance [1–6] since correlations are enhanced by the reduced dimensionality. They also offer the advantage to access, in some special cases, the exact many-body wave function. For instance, homogeneous 1D quantum systems with a well-defined symmetry can be solved via the Bethe ansatz [7–15]). However, it is well known that correlation functions often remain very difficult to extract due to the complexity of the Bethe ansatz equations and the resulting many-body wave function.

One special case that allows to go further in the calculations, capturing correlation functions [16–19] and dynamics [20–23], even in the presence of external confinements, is the Tonks-Girardeau (TG) limit [7], where the interaction strength is repulsive and tends to infinity. The study of this limiting case allows a deep understanding of quantum correlations in many-body systems [24–26] in and out of equilibrium, and to have a benchmark for numerical simulations of such systems.

The ground state of such TG quantum mixtures is highly degenerate due to exchange symmetry of particles. Indeed, at zero temperature, any arrangement of the particles has the same energy. On the other hand, in an actual experiment, interaction between particles although potentially large always remain finite, and consequently the macroscopic degeneracy is lifted and the lowest-energy state is generally unique and corresponds, for the spatial part, to the most symmetric possible state [17,27].

In this article we show that the ground state for a 1D strongly interacting mixture depends on the protocol used to approach the TG regime. We consider a two-component bosonic mixture and we analyze two cases: the SU(2) case where the intra- and interspecies interactions are equal and very large, and the symmetry-breaking case (SB) where the intraspecies interactions are diverging and the interspecies interaction is increased afterwards. In the first case the many-body ground state is identical to that of a single-component TG gas: the spatial symmetry is the highest, and the two spin components are strongly correlated even at large distance because, due to the symmetry, it is as if there was no spin at all. In the SB case, we show that the distinguishability introduced by the difference between the inter- and intraspecies interaction strengths, even if it slightly affects the symmetry of the many-body wave function, makes the spin correlation to drastically drop.

The paper is organized as follows. The model is presented in Sec. II. Here we provide a physical discussion about the difference between the SU(2) and the SB cases, in order to guide the reader to the physical comprehension of the results obtained in this work. In Sec. III we discuss in detail our procedure to obtain the ground-state many-body wave function for the SU(2) Hamiltonian and for the SB one. We quantify the breaking of the symmetry associated to the SB many-body ground state by calculating the expectation value of the two-cycle-sum operator in Sec. IV. We show that for large number of particles, the SB state is halfway between the most symmetric and the most antisymmetric states allowed by the SU(2) Hamiltonian. Correlations are analyzed starting from Sec. V. We calculate the momentum distribution that is given

 ©2022 American Physical Society

by the Fourier transform of the one-body density matrix. In Secs. VI and VII we study the zero-mode occupation number and the Tan's contact. The first is related to long-distance correlations and the second to short-distance correlations. In Sec. VIII some remarks on the relation between our approach and the Bethe ansatz solution conclude the paper.

II. THE MODEL: PHYSICAL DISCUSSION

We consider a balanced two-components 1D Bose gas, characterized by contact interactions, in a ring geometry (periodic boundary conditions) at zero temperature. The two components are labeled by an index $\sigma = \uparrow, \downarrow$ for convenience but this index has no relation with the spin one-half of fermions. The general Hamiltonian for N bosons reads

$$\hat{H} = \sum_{\sigma=\uparrow,\downarrow} \sum_{i}^{N_\sigma} \left[-\frac{\hbar^2}{2m} \frac{\partial^2}{\partial x_{i,\sigma}^2} + g_{\sigma\sigma} \sum_{j>i}^{N_\sigma} \delta(x_{i,\sigma} - x_{j,\sigma}) \right] + g_{\uparrow\downarrow} \sum_{i}^{N_\uparrow} \sum_{j}^{N_\downarrow} \delta(x_{i,\uparrow} - x_{j,\downarrow}) \tag{1}$$

with $g_{\uparrow\downarrow}$ the interspecies, $g_{\uparrow\uparrow}$ ($g_{\downarrow\downarrow}$) the intraspecies interaction strengths, and $N_\downarrow = N_\uparrow = N/2$ the number of particle per component. The aim of this work is to analyze the ground-state coherence properties of the symmetry-breaking case with $g_{\uparrow\uparrow} = g_{\downarrow\downarrow} \neq g_{\uparrow\downarrow}$ with respect to those of the SU(2) case with $g_{\uparrow\uparrow} = g_{\downarrow\downarrow} = g_{\uparrow\downarrow}$.

In particular we are interested in the strongly interacting regime where all interaction strengths diverge in the SU(2) case, and where, in the SB case, $g_{\sigma\sigma} \to \infty$ and $g_{\uparrow\downarrow}$ is very large but finite.

Since in the experiments infinite quantities do not exist, both situations could seem just different experimental protocols leading to the same Hamiltonian, where intraspecies and interspecies interactions approach the TG regime. However, in the first protocol the interaction strengths are equal and simultaneously driven towards the strong-interaction regime. On the other hands, in the second protocol, the intra- and interspecies interactions are different: they are driven towards large values in two consecutive times or in a different manner. The differences between these two different protocols strongly affect the properties of the ground state.

In the TG limit, the ground state is highly degenerate since each particle distribution along the ring has the same energy. The choice of the experimental protocol used to reach this limit will select a specific state of the manifold. In the SU(2) case, the selected state will correspond to the ground state for the case of large, but finite, equal intra- and interspecies interactions. In the SB case the selected state will correspond to the ground state for a two-component TG gas where the interspecies interaction is large but finite.

In the first case, because of the SU(2) symmetry and thus of the indistinguishability of the two spin components, we expect the ground state to be the same as that of a single-component TG gas. Indeed, such a system can be mapped on a XXX-spin chain [22], whose ground state for bosons is ferromagnetic with the largest possible spin value ($s = N/2$), namely, the many-body wave function will be fully symmetric. Consequently, all the observables for the SU(2) ground state will be the same as for a single-component TG.

The second case is rather close to a balanced SU(2) fermionic gas, except for the symmetry with respect to the exchange of particles having the same spin. In the ground state, we expect alternating spin arrangements to be energetically favorable, due to the difference between the intraspecies (infinite) and interspecies (very large but finite) interactions. Indeed, for the SU(2) fermionic case, one would have an antiferromagnetic ground state. For the bosonic case studied in this work, the bosonic nature of each component breaks the SU(2) symmetry: the system can be mapped on XXZ-spin chain (Appendix B), whose Hamiltonian does not commute with the spin operator $\vec{S}^2$. The expectation value for such operator will be necessarily lower than that for the SU(2) case, thus the many-body wave function will not be fully symmetric.

We expect two main consequences on the difference between the momentum distributions of the two systems. The first is that the zero-mode occupation (large-distance correlations) drops by a factor of two (in the thermodynamic limit) in the SB case with respect to the SU(2) one. The distinguishability of the two spin components and the balanced population of the components make the probability to find a particle of the same spin, at large distance, to be one half with respect to the SU(2) case. The second consequence is a decrease in the Tan's contact (short-distance correlations). This observable is proportional to the symmetric exchanges among the particles [18]. The many-body wave function being less symmetric, the Tan's contact will be lower too with respect to the SU(2) case.

The following sections will be devoted to the rigorous proof of our conjectures.

III. THE GROUND-STATE SOLUTION IN THE STRONGLY INTERACTING LIMIT

In the limit $g_{\sigma\sigma'} \to +\infty$, for any σ, σ', the many-body wave function vanishes whenever $x_i = x_j$ (from now on we drop the spin index in the particle positions). Thus, it can be written in terms of linear combinations of fermionic wave functions [20,28]

$$\Psi(x_1, \ldots, x_N) = \sum_{P \in S_N} a_P \theta_P(x_1, \ldots, x_N) \Psi_S(x_1, \ldots, x_N), \tag{2}$$

where S_N is the permutation group of N elements, P a permutation operator, $\theta_P(x_1, \ldots, x_N)$ is equal to 1 in the coordinate sector $x_{P(1)} < \cdots < x_{P(N)}$. The wave function $\Psi_S = A\Psi_A$ is given by the action of the unit antisymmetric function $A = \prod_{i<j} \mathrm{sgn}(x_i - x_j)$ on the fully antisymmetric fermionic wave function,

$$\Psi_A = \frac{1}{\sqrt{N!}} \det\left[\phi_m(x_n)\right], \tag{3}$$

where $\phi_m(x_n) = e^{ik_m x_n}/\sqrt{L}$ with $k_m = \pi(2m - N - 1)/L$ and $n, m \in 1, \ldots, N$, $\forall x_n \in [-L/2, L/2]$, for particles on a ring of length L. The rules for exchanging identical particles being fixed by the statistics, we can restrict our basis to $N!/(\frac{N}{2}!\frac{N}{2}!)$ independent sectors (and then a_P) instead of the $N!$ possible. These sectors represent all the possible spins configurations and are usually called snippets [16]. They constitute the

proper basis to describe a two-component spin mixture and will be used through this paper.

In this work we focus on the ground-state solution that is not degenerate for balanced mixtures (in the limit $g_{\sigma\sigma'}$ very large but finite), so that we can set a_P real without loss of generality, and use a strong-coupling expansion by calculating the energy to first order with respect to the small parameters $1/g_{\sigma\sigma'}$.

A. The SU(2) case

We first recall the method for the case of a SU(2) boson gas with $g_{\uparrow\downarrow} = g_{\uparrow\uparrow} = g_{\downarrow\downarrow} = g$. The two-spin components being indistinguishable, we expect the ground state to be equivalent to that of a one-component TG gas. In such a case all the a_P are equal in each sector.

The minimization of the energy in the limit $g \to \infty$,

$$E_g \simeq E_\infty + \frac{1}{g}[\partial_{1/g} E]_{g\to\infty} = E_\infty - \frac{1}{g}K, \tag{4}$$

corresponds to the maximization of the energy slope $K = -[\partial_{1/g} E]_{g\to\infty}$. The procedure is analogous to that outlined in [17]. One writes K as a function of the a_P coefficients,

$$K(a_P) = \frac{\hbar^4}{m^2}\left(\sum_{P,Q\in S_N} (a_P + a_Q)^2 \alpha_{P,Q} + 2\sum_{P,P'\in S_N} a_{P'}^2 \alpha_{P,P'}\right), \tag{5}$$

and then finds the stationary solutions of this function taking into account the normalization condition $\sum_P a_P^2 = 1$. The terms $\alpha_{P,Q}$ in Eq. (5) are the nearest-neighbor exchange constants, given by the relation

$$\alpha_{P,Q} = N! \int dx_1, \ldots dx_N \theta_{\mathrm{Id}}(x_1, \ldots, x_N)\delta(x_k - x_{k+1})\left(\frac{\partial \Psi_A}{\partial x_k}\right)^2 \equiv \alpha_k \tag{6}$$

if P and Q (P and P') are equal up to a transposition of two consecutive distinguishable particles (indistinguishable bosons), and $\theta_{\mathrm{Id}}(x_1, \ldots, x_N)$ is the indicator of the sector $x_1 < \cdots < x_N$.

In a ring geometry, at fixed number of particle N, all the α_k are the same, $\alpha_k = \alpha^{(N)}$, $\forall k$, because of the homogeneity of the potential. In order to calculate $\alpha^{(N)}$, we consider one of the variables (here x_1) as a moving boundary for the other $N-1$ ones. This leads to

$$\alpha^{(N)} = (N-1)! \int_0^L dx_1 \prod_{i=2}^{N} \int_{x_{i-1}}^{x_1+L} dx_i \delta(x_1 - x_2)\left|\frac{\partial \Psi_A}{\partial x_1}\right|^2 = \frac{N(N^2-1)}{3L^3}\pi^2. \tag{7}$$

In agreement with [29], we find that $\alpha^{(N)}$ is equal to twice the kinetic energy up to a dimensional constant, the sum of $k_m^2 L^2$ over the occupied orbitals being equal to $N(N^2-1)\pi^2/3$.

The conditioned maximization of $K(a_P)$ is equivalent to solving the eigenvalue problem for a matrix V whose form depends on the type of mixture and trapping potential. In the bosonic SU(2) case,

$$[V^{\mathrm{SU}}]_{i,j} = \frac{\hbar^4}{m^2}\begin{cases} \sum_{d,k\neq i} \alpha_{i_k} + 2\sum_{b,k\neq i} \alpha_{i_k} & j = i \\ \alpha_{i,j} & j \neq i \end{cases}, \tag{8}$$

where the d-sum has to be taken over snippets k that transpose distinguishable particles, while the b-sum runs over sectors that transpose identical bosons. The explicit form of V^{SU} for the case of a mixture of $2+2$ bosons is given in Appendix A. We remark that the positive sign of the off-diagonal part as well as the plus in Eq. (5) depend on the choice made while building the many-body wave function in Eq. (2), namely, on the choice to start with Ψ_S or Ψ_A.

The largest eigenvalue of this matrix,

$$K^{\mathrm{SU}} = \left[\vec{a}_P^{\mathrm{SU}}\right]^t V^{\mathrm{SU}} \vec{a}_P^{\mathrm{SU}}, \tag{9}$$

$\vec{a}_P^{\mathrm{SU}}$ being the eigenvector of V^{SU} corresponding to this eigenvalue, can be written under the form $K^{\mathrm{SU}} = K_{\uparrow\downarrow}^{\mathrm{SU}} + \sum_{\sigma=(\uparrow,\downarrow)} K_{\sigma\sigma}^{\mathrm{SU}}$, highlighting the inter- and intracomponent contributions to the energy. Finally, we obtain $K^{\mathrm{SU}} = 2N\alpha^{(N)}\hbar^4/m^2$.

B. The symmetry-breaking case

We now move to the more complicated case of two interacting TG gases, where $g_{\uparrow,\uparrow}$ and $g_{\downarrow,\downarrow}$ are infinite and the intercomponent interaction strength $g_{\uparrow,\downarrow}$ is very large, but finite. The minimization procedure, outlined in Eq. (4), with respect to the small parameter $1/g_{\uparrow,\downarrow}$ leads to a matrix V^{SB} that does not take into account any intracomponent interaction terms:

$$[V^{\mathrm{SB}}]_{i,j} = \frac{\hbar^4}{m^2}\begin{cases} \sum_{d,k\neq i} \alpha_{i_k} & j = i \\ \alpha_{i,j} & j \neq i \end{cases}. \tag{10}$$

Remark that the largest eigenvalue of V^{SB}, denoted as $K_{\uparrow\downarrow}^{\mathrm{SB}}$ as well as the other eigenvalues, gives only an intercomponent contribution to the energy, as $g_{\sigma\sigma}$ has been sent to infinity from the beginning. Of course the symmetry breaking occurs for $N > 2$, as no intrainteraction occurs for the case $N_\uparrow = N_\downarrow = 1$. Again, the explicit form of V^{SB} for the case of a mixture of $2+2$ bosons is given in Appendix A.

We note that V^{SB} is very similar to the matrix V_F^{SU} for a SU(2) fermionic mixture. Indeed, $[V_F^{\mathrm{SU}}]_{i,i} = [V^{\mathrm{SB}}]_{i,i}$, and $[V_F^{\mathrm{SU}}]_{i,j} = -[V^{\mathrm{SB}}]_{i,j}$ if $i \neq j$. The two matrices have the same eigenvalues, but the eigenstates do not have the same symmetry, which is well defined for the case of SU(2) fermions but is not, as we will see in the next section, for the case of two interacting TG gases. Let us point out that, because of our basis choice, V^{SU} and V_F^{SU} can be mapped on a XXX spin-chain model [22], while V^{SB} can be mapped on an XXZ model (Appendix B).

IV. ANALYSIS OF THE SYMMETRY BREAKING

We now explain how to characterize the symmetry properties of the two different ground states using irreducible representations of the permutation group S_N. We will show in this section that the ground state of the SU(2) Hamiltonian has a well-defined symmetry whereas the one of the symmetry-breaking case does not. In order to quantify the symmetry breaking associated with the many-body state

$$\Psi^{\mathrm{SB}}(x_1, \ldots, x_N) = \sum_{P\in S_N} a_P^{\mathrm{SB}} \theta_P(x_1, \ldots, x_N)\Psi_S(x_1, \ldots, x_N), \tag{11}$$

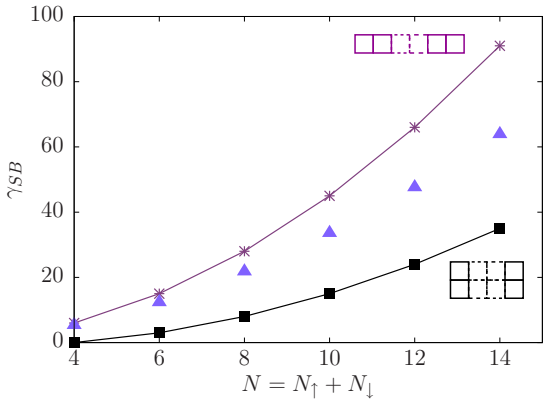

FIG. 1. γ_{SB} as a function of N (triangles) for the symmetry-breaking ground state. The stars and the boxes represent the eigenvalues $\gamma_S^{(2)}$ and $\gamma_A^{(2)}$, respectively. The lines are guide to the eye.

we calculate the expectation value of the two-cycle class-sum operator $\Gamma^{(2)} = \sum_{i<j}(i, j)$ [30,31], whose eigenvalues are directly connected to the irreducible representations of S_N, and thus to a Young tableau. Indeed, the relation between the eigenvalues $\gamma^{(2)}$'s and a Young tableau with a number of boxes λ_i at line i is

$$\gamma^{(2)} = \frac{1}{2}\sum_i [\lambda_i(\lambda_i - 2i + 1)]. \tag{12}$$

Thus, for the fully symmetric SU(2) ground state, corresponding to the Young tableau $(N) = \square\square\square\cdots\square\square\square$, one has $\gamma_S^{(2)} = N(N-1)/2$, namely, $\gamma_S^{(2)}$ is given by the number of pairs in a system of N particles. Instead the antisymmetric eigenvalue $\gamma_A^{(2)}$, corresponding to the Young tableau $(N/2, N/2) = \begin{smallmatrix}\square\square\\\square\square\end{smallmatrix}\cdots\begin{smallmatrix}\square\square\\\square\square\end{smallmatrix}$, is equal to $N(N-4)/4$. This corresponds to the number of pairs in a system of $N/2$ particles (the length of a row) minus $N/2$ (the number of columns).

The operator $\Gamma^{(2)}$ can be written as a function of the spin operator $\vec{S}^2$. Indeed, it can be shown that for a balanced mixture $\Gamma^{(2)} = \vec{S}^2 + \frac{N(N-4)}{4}\mathbb{1}$ (Appendix D). This means that $\gamma_S^{(2)}$ corresponds to a total spin $s = N/2$, and $\gamma_A^{(2)}$ to $s = 0$.

In Fig. 1 we plot $\gamma_{SB} = \langle\Psi^{\rm SB}|\Gamma^{(2)}|\Psi^{\rm SB}\rangle$ as a function of N, and we compare it with $\gamma_S^{(2)}$ and $\gamma_A^{(2)}$. We observe that, by increasing N, γ_{SB} moves away from $\gamma_S^{(2)}$ to position itself halfway between $\gamma_S^{(2)}$ and $\gamma_A^{(2)}$. We have checked that the corresponding symmetry-breaking ground state ($\vec{a}_P^{\rm SB}$) does not correspond to any well-defined symmetry, and thus to any well-defined spin. The explicit calculation for the case of $N = 4$ bosons is given in Appendix C. The formal demonstration of the symmetry breaking is given in Appendix E.

V. CORRELATION ANALYSIS

The previous analysis allowed us to demonstrate that the precise protocol used in an experiment to set particle interactions to very large value has strong consequences on the symmetry properties of the ground state. However, the exchange symmetry, or the expectation of the two cycle class sum operators are not accessible experimentally. We therefore now look for a routinely measured physical observable that would keep trace of the nontrivial symmetry of the ground state. The simplest one that strongly depends on the symmetry of the wave function is the momentum distribution, obtained from the Fourier transform of the one-body density matrix. This statement is, for instance, obvious for noninteracting bosons and fermions which have completely different momentum distributions (Fermi-Dirac step function for fermions and Bose-Einstein distribution for bosons) but can be generalized to interacting mixtures with nontrivial symmetries under exchange of particles [18,19]. Starting from the many-body wave function, the one-body density matrix is obtained as follows:

$$\rho_1(x, y) = N\int dx_2, \ldots, dx_N \Psi^*(x, x_2, \ldots, x_N) \times \Psi(y, x_2, \ldots, x_N), \tag{13}$$

that, for a multicomponent system, can be written [22]

$$\rho_1(x, y) = \sum_\sigma N_\sigma \rho_{1,\sigma}(x, y), \tag{14}$$

where

$$\rho_{1,\sigma}(x, y) = \sum_{i,j=1}^{N} c_\sigma^{(i,j)} \rho^{(i,j)}(x, y). \tag{15}$$

This representation is very useful as it separates spin and orbital correlations. Indeed, the term in Eq. (15)

$$\begin{aligned}\rho^{(i,j)}(x, y) = \theta(x, y)N! \int_{x_1<\cdots<x_{i-1}<x<x_{i+1}<\cdots<x_j<y<x_{j+1}<\cdots<x_N} \\ \times dx_1 \cdots dx_{i-1} dx_{i+1} \cdots dx_N \\ \times \Psi_S^*(x_1, \ldots, x_{i-1}, x, x_{i+1}, \ldots, x_N) \\ \times \Psi_S(x_1, \ldots, x_{i-1}, y, x_{i+1}, \ldots, x_N),\end{aligned} \tag{16}$$

where $\theta(x, y)$ is equal to 1 if $x \leqslant y$ and $i \leqslant j$, and 0 otherwise [22], is the contribution to the reduced one-body density matrix calculated on the sector

$$x_1 < \ldots < x_{i-1} < x < x_{i+1} < \ldots < x_j < y < x_{j+1} < \ldots < x_N.$$

The $y < x$ part of the correlation function can be obtained using the symmetry relation $\rho^{(i,j)}(x, y) = \rho^{(j,i)}(y, x)$. The term

$$c_\sigma^{(i,j)} = \sum_{k=1}^{(N-1)!} a_{i(\sigma)k} a_{j(\sigma)k} \tag{17}$$

is the spin weight related to the contribution (16). The amplitudes $a_{i(\sigma)k}$ in Eq. (17) are now labeled with respect to the position of the ith particle ($i = 1, \ldots, N$) with spin σ and consider all the $k = 1, \ldots, (N-1)!$ permutations of the $N-1$ other particles. Remarkably, both the SU(2) and the SB systems have the same spatial correlation function $\rho^{(i,j)}(x, y)$. The symmetry properties affect only the spin correlation function $c_\sigma^{(i,j)}$.

As we are focusing on the special case of a ring that is invariant for translation symmetry, in the following we will set $\rho_1(x, y) = \rho_1(x - y) = \rho_1(t)$ and $\rho_{1,\sigma}(x, y) = \rho_{1,\sigma}(x - y) = \rho_{1,\sigma}(t)$. From an experimental point of view, one has easily access the momentum distribution, which is given by

$$n(k) = \int_{-L/2}^{L/2} e^{-ikt}\rho_1(t)\, dt. \tag{18}$$

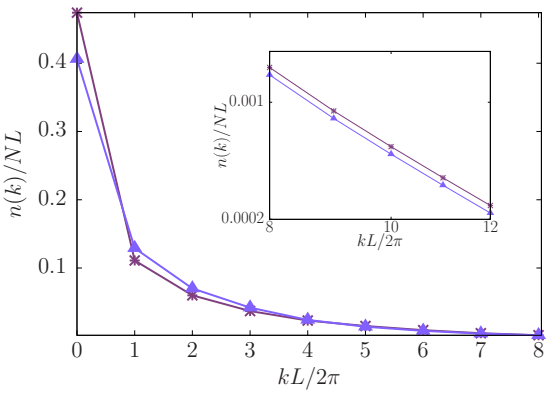

FIG. 2. Normalized momentum distribution $n(k)/N$ in units of $1/L$ as a function of $kL/(2\pi)$ for a mixture of $4+4$ bosons. The stars are the data for the SU(2) mixture and the triangles for the SB system. The inset, in a log-log scale, is a zoom on the tails. The lines are guide to the eye.

In Fig. 2 we compare the momentum distribution for the SB mixture with that of the ground state for a SU(2) mixture, the latter coinciding with the momentum distribution of a single component TG gas. We notice remarkable differences among the two both at small and at large momenta. In particular, both the peak centered around $k = 0$ and the tails at large k (inset of Fig. 2) of the momentum distribution are larger for the SU(2) mixture, while the one of the SB mixture is higher at intermediate wave vectors. Thus, in the following sections we will focus our study on $n_0 = n(k = 0)$ and $\lim_{k\to\infty} n(k)$, which provide information about large- and short-distance correlations, respectively. Moreover, in the ring geometry, n_0 coincides with the quasicondensate fraction of the system.

VI. LARGE-DISTANCE CORRELATIONS

We now discuss in detail the large-distance correlations which corresponds to small momenta in the momentum distribution. Specifically, we restrict this analysis to the zero-momentum occupation number, which is an important measure of long-range coherence in quantum systems. For the balanced mixture discussed in this paper $\rho_{1,\sigma}(x, y)$ is independent of σ, so n_0 is given by

$$n_0 = \int_{-L/2}^{L/2} dt\ \rho_1(t) = 2\sum_{j=1}^{N/2} c_{1j} R^j, \tag{19}$$

where we have defined $R^j = \int_{-L/2}^{L/2} dt\ \rho^{(1,j)}(t)$ and we have used that $c_{1,j} = c_{1,(N-j+1)}$. We are mostly interested in the asymptotic behavior at large number of particles that we approach by increasing the number of particles up to $N = 14$. The results of our exact calculations are actually well approximated by a simple fitting function R^j at large number of particles,

$$R^j \underset{N\to\infty}{\simeq} \frac{3}{4}\frac{1}{\sqrt{2j-1}}. \tag{20}$$

For the SU(2) case, $c_{1,j} = 1, \forall j$. This implies that the ground state of the SU(2) system coincides with that of a TG gas with a single spin component. Indeed, if there was only one spin component, the spin correlation function would be maximum $\forall j$. The resulting approximated expression for the zero-momentum occupation, in the limit $N \gg 1$, reads

$$n_0^{\mathrm{SU}}(N \gg 1) \simeq \frac{3}{2}\sum_{j=1}^{N/2} \frac{1}{\sqrt{2j-1}}. \tag{21}$$

This approximation Eq. (21) provides the correct leading term of the function $n_0^{\mathrm{SU}}(N)$ given in [32] for a single-component TG gas,

$$n_0^{\mathrm{SU}}(N) = 1.54\sqrt{N} - 0.58 + \frac{0.03}{\sqrt{N}}. \tag{22}$$

For the SB case, the c_{1j} depend on N for small values of N but they seem to converge rapidly to a well defined value c_{1j} for any j (see Table I). Breaking the SU(2) symmetry makes the two spin states distinguishable. Thus, we expect that, at large j, there are no more correlations between the first spin and the jth one, so that the probability c_{1j} to have the same spin state has to tend to $1/2$. Indeed, the c_{1j} can be fitted with the function

$$f_{1j} = \left(\tfrac{1}{2} + \tfrac{1}{2}e^{-b(j-1)^a}\right), \tag{23}$$

a and b being positive and slightly depending on N. The exponential decay part of Eq. (23) does not contribute in the thermodynamic limit, so that

$$\lim_{N\to\infty} \frac{n_0^{\mathrm{SB}}}{n_0^{\mathrm{SU}}} = \frac{1}{2}. \tag{24}$$

In Fig. 3 we plot the exact results for n_0^{SU} and n_0^{SB}, together with the analytical approximated expression for $n_0^{\mathrm{SU}}(N)$ given in Eq. (22) and that for the symmetry-breaking case,

$$n_0^{\mathrm{SB}}(N) = 0.77\sqrt{N} + 1.64 - \frac{1.61}{\sqrt{N}}. \tag{25}$$

Equation (25) has been obtained by fitting the data obtained by the exact calculation and by fixing the first coefficient to 0.77 [half the first coefficient of Eq. 22)].

Breaking the SU(2) symmetry has therefore the tendency to destroy long-range coherence. For our particular model, the zero-momentum occupation number is reduced by a factor of two. This macroscopic consequence of a microscopic symmetry property is a central result of this paper as it constitutes an experimental smoking gun of SU(2) symmetry breaking.

TABLE I. Behavior of the absolute value of the coefficients c_{1j} as functions of N for the case of breaking symmetry.

$N/2$	c_{12}	c_{13}	c_{14}	c_{15}	c_{16}	c_{17}	c_{18}
2	0.833						
3	0.811	0.769					
4	0.804	0.750	0.721				
5	0.801	0.742	0.702	0.687			
6	0.799	0.737	0.692	0.671	0.660		
7	0.798	0.735	0.687	0.662	0.645	0.638	
8	0.797	0.733	0.683	0.656	0.636	0.625	0.619

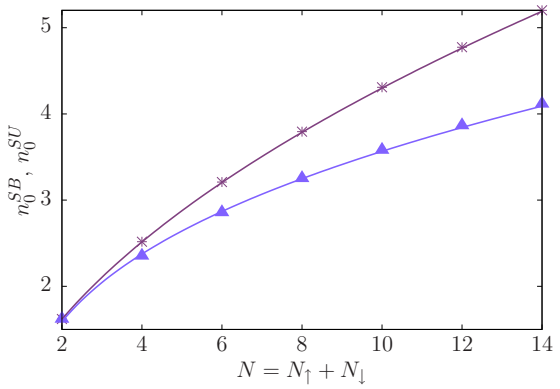

FIG. 3. The zero-momentum occupation numbers n_0^{SU} (stars) and n_0^{SB} (triangles), for a balanced mixture, as a function of the total number of particles N. The exact results (points) are compared with the approximated function (lines) given respectively in Eq. (22) and Eq. (25).

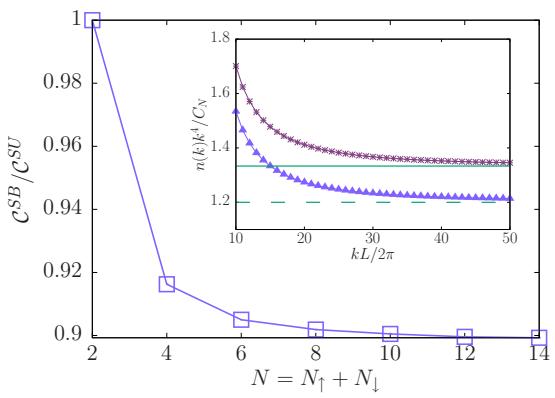

FIG. 4. The ratio $\mathcal{C}^{\mathrm{SB}}/\mathcal{C}^{\mathrm{SU}}$ as a function of $N = N_\uparrow + N_\downarrow$ for balanced mixtures (the line is a guide to the eye). In the inset we show $N(k)k^4$, in units of $C_N = N^2(N^2-1)/L^3$, as a function of $kL/(2\pi)$ for the case of a SU(2) mixture (stars) and a SB one (triangles) of $N = 4+4$ bosons. The horizontal lines indicates the values of $\mathcal{C}^{\mathrm{SU}}/C_N$ (continuous line) and $\mathcal{C}^{\mathrm{SB}}/C_N$ (dashed line).

VII. SHORT-DISTANCE CORRELATIONS: THE TAN'S CONTACT

We now proceed with the discussion of short-distance correlations. This time, they are observable in the tails of the momentum distribution. For a system with zero-range interactions, the momentum distribution decays as k^{-4}. The prefactor $\mathcal{C} = \lim_{k\to\infty} n(k)k^4$ is the so-called Tan's contact [33]. This observable is proportional to the number of derivative discontinuities (cusps) in the systems, namely, to the symmetric exchanges between particles [18,19]. In this section we will focus on the modification of the Tan's contact due to symmetry breaking.

For the SU(2)-symmetric system, the Tan's contact is proportional to the energy slope K^{SU},

$$\mathcal{C}^{\mathrm{SU}} = \frac{2m^2}{\hbar^4} K^{\mathrm{SU}}. \tag{26}$$

In the ring geometry for the SU(2) case, there are N cusps, and each cusp brings a contribution that is proportional to twice $\alpha^{(N)}$, so that $K^{\mathrm{SU}} = 2N\alpha^{(N)}\hbar^4/m^2$ and thus $\mathcal{C}^{\mathrm{SU}} = 4N\alpha^{(N)}$.

For the SB case, $K^{\mathrm{SB}}_{\uparrow\downarrow}$ takes into account only the intercomponent contribution, as our starting point in the energy calculation is a two-component TG gas whose intraspecies interaction strength is set to infinity from the beginning. However, the Tan's contact is related to both the intra- and intercomponent contributions $[\partial_{1/g_{\sigma,\sigma}} E]_{g_{\sigma,\sigma}\to\infty}$ and $[\partial_{1/g_{\sigma,\sigma'}} E]_{g_{\sigma,\sigma'}\to\infty}$, the first term counting the cusps for exchange of identical bosons, and the second giving the cusps for exchange of bosons with different spins. Specifically, in the SB case the contact is given by (see Appendix F for derivation)

$$\mathcal{C}^{\mathrm{SB}} = \frac{2m^2}{\hbar^4}\left[\left(\vec{a}_P^{\mathrm{SB}}\right)^t V^{\mathrm{SU}} \vec{a}_P^{\mathrm{SB}}\right] \tag{27}$$

with $\vec{a}_P^{\mathrm{SB}}$ being the eigenvector of V^{SB} corresponding to its largest eigenvalue.

In Fig. 4 we plot the ratio $\mathcal{C}^{\mathrm{SB}}/\mathcal{C}^{\mathrm{SU}}$ as a function of N. We observe that $\mathcal{C}^{\mathrm{SB}}/\mathcal{C}^{\mathrm{SU}}$ converges very rapidly to $\sim$0.9. Thus, for $N > 2$, the contact is lower for the SB case than for the SU(2) mixture. As reported for other multicomponent mixtures [18], the reduction of the symmetry also manifests itself in the lowering of the contact in this case. The fact that the change is relatively small is due to the fact that each component of the mixture is bosonic and, then, the most of the particles exchanges are still symmetric even in the SB case.

VIII. CONCLUDING REMARKS

In this paper we have presented a model of a boson-boson mixture where exchange symmetry is broken and obtained its solutions at large interparticle interaction. Before summing up our conclusions, we would like to mention that the solution of such a model can also be obtained, for any strength of the interparticle interaction, by means of the Bethe ansatz solution for the Yang-Gaudin Hamiltonian [14]. Indeed one can write, in each coordinate sector Q such that $x_{Q(1,\uparrow)} < \cdots < x_{Q(N,\downarrow)}$,

$$\Psi_Q^{\mathrm{SB}}(x_1,\ldots,x_N) = \prod_{i,j}\prod_{\sigma=\uparrow,\downarrow} \mathrm{sgn}(x_{Q(i,\sigma)} - x_{Q(j,\sigma)}) \times \Psi_Q^{\mathrm{YG}}(x_1,\ldots,x_N), \tag{28}$$

where the function Ψ_Q^{YG} is the Bethe wave function for the SU(2) Fermi gas in the coordinate sector Q. The great advantage of our method, which is exact up to the order $1/g_{\uparrow\downarrow}$, is the ease with which one can access the one-body correlation function, allowing a deep understanding of spatial and spin correlations. Another important advantage of the method outlined in this work is that it can be applied to any trapping potential. As soon as one knows the single-particle orbitals, such as for the case of a harmonic potential or a box trap, it is possible to write the exact solution for the many-body wave function for the symmetry-breaking case too.

In particular, in this work, we have shown that different spin states with different symmetries can be obtained by

varying the protocol used in order to achieve the strong-repulsive limit. The symmetry breaking induced by the difference between the intra- and interspecies interaction strengths affects both short- and large-distance correlations, but the effect on the large-distance correlations is more dramatic. Indeed, at large number of particles we observe a depletion by a factor two of the zero-momentum occupation number, which is a signature of a lack of spin correlation at large distance. This means that the zero-momentum occupation number is a very sensitive observable for detecting symmetry breaking.

Our work provides a guide for the studies of the correlation properties of SU(κ) mixtures in the strongly interacting regime, highlighting the importance of the protocol chosen to reach such a regime.

ACKNOWLEDGMENTS

G.A.-D. acknowledges Manon Ballu and Martial Morisse for fruitful discussions, and all authors acknowledge Hélène Perrin for important comments on the symmetry analysis. We acknowledge funding from the ANR-21-CE47-0009 Quantum-SOPHA project.

APPENDIX A: THE MATRICES V^{SU} AND V^{SB}

Here we will give the explicit example for the calculation of V^{SU} and V^{SB} for the case of a balanced mixture with $N = 4$ bosons. We consider the snippet basis $\{\uparrow\uparrow\downarrow\downarrow, \uparrow\downarrow\uparrow\downarrow, \uparrow\downarrow\downarrow\uparrow, \downarrow\uparrow\uparrow\downarrow, \downarrow\uparrow\downarrow\uparrow, \downarrow\downarrow\uparrow\uparrow\}$. For the SU(2) mixture in a ring geometry, the V^{SU} matrix reads

$$V^{\mathrm{SU}} = \frac{\hbar^4}{m^2}\alpha^{(N)}\begin{pmatrix} 6 & 1 & 0 & 0 & 1 & 0 \\ 1 & 4 & 1 & 1 & 0 & 1 \\ 0 & 1 & 6 & 0 & 1 & 0 \\ 0 & 1 & 0 & 6 & 1 & 0 \\ 1 & 0 & 1 & 1 & 4 & 1 \\ 0 & 1 & 0 & 0 & 1 & 6 \end{pmatrix}, \tag{A1}$$

whose largest eigenvalue is $8\hbar^4\alpha^{(N)}/m^2$ with corresponding eigenvector $\vec{a}_P^{\mathrm{SU}} = \frac{1}{\sqrt{6}}(1, 1, 1, 1, 1, 1)$.

For the SB mixture, the V^{SB} matrix reads

$$V^{\mathrm{SB}} = \frac{\hbar^4}{m^2}\alpha^{(N)}\begin{pmatrix} 2 & 1 & 0 & 0 & 1 & 0 \\ 1 & 4 & 1 & 1 & 0 & 1 \\ 0 & 1 & 2 & 0 & 1 & 0 \\ 0 & 1 & 0 & 2 & 1 & 0 \\ 1 & 0 & 1 & 1 & 4 & 1 \\ 0 & 1 & 0 & 0 & 1 & 2 \end{pmatrix}. \tag{A2}$$

The largest eigenvalue is $6\hbar^4\alpha^{(N)}/m^2$ and its corresponding eigenvector reads $\vec{a}_P^{\mathrm{SB}} = \frac{1}{2\sqrt{3}}(1, 2, 1, 1, 2, 1)$.

It is worth making the case $N = 2$ explicitly. Indeed, because of the periodic boundary conditions, the $\delta(x_1 - x_2)$ contributes twice both for the diagonal terms and the off-diagonals ones. Thus, on the snippet basis $\{\uparrow\downarrow, \downarrow\uparrow\}$, one has the matrix

$$V^{\mathrm{SU}} = V^{\mathrm{SB}} = \frac{\hbar^4}{m^2}\alpha^{(N)}\begin{pmatrix} 2 & 2 \\ 2 & 2 \end{pmatrix}, \tag{A3}$$

whose largest eigenvalue is $4\alpha^{(N)}\hbar^4/m^2$, in agreement with $K^{\mathrm{SU}} = 2N\alpha^{(N)}\hbar^4/m^2$.

APPENDIX B: MAPPING ON THE *XXX* SPIN-CHAIN MODEL FOR SU(2) MIXTURES

In the strong-interacting limit, in the case of SU(2) bosons or fermions, the Hamiltonian (1) can be mapped into a spin-chain model. Indeed, at the order $1/g$ one can write [20]

$$\hat{H} - \mathbb{1}E_{g\to\infty} = -V_{B,F}^{\mathrm{SU}}/g = -NJ\mathbb{1} \mp J\sum_{j=1}^{N}\hat{P}_{j,j+1}, \tag{B1}$$

where $J = \alpha^{(N)}/g$, the $-$ $(+)$ sign applies to bosons (fermions). Since the permutation operator $\hat{P}_{j,j+1}$ can be written as a function of product of Pauli matrices $\hat{P}_{j,j'} = (\vec{\sigma}^{(j)} \cdot \vec{\sigma}^{(j')} + \mathbb{1})/2$ acting on site j and j', it is straightforward to show that it is possible to map (B1) on a Heisenberg XXX chain model, for both bosons and fermions: a ferromagnetic one for SU(2) bosons,

$$-\frac{V_B^{\mathrm{SU}}}{g} = -2J\sum_{j=1}^{N}\vec{S}^{(j)} \cdot \vec{S}^{(j+1)} - \tfrac{3}{2}NJ\mathbb{1}, \tag{B2}$$

and an antiferromagnetic one for SU(2) fermions,

$$-\frac{V_F^{\mathrm{SU}}}{g} = 2J\sum_{j=1}^{N}\vec{S}^{(j)} \cdot \vec{S}^{(j+1)} - \tfrac{1}{2}NJ\mathbb{1}, \tag{B3}$$

where $\vec{S} = \vec{\sigma}/2$ are the spin operators.

For the SB case the Hamiltonian can be written

$$\begin{aligned}\hat{H} - \mathbb{1}E_{g\to\infty} &= -V^{\mathrm{SB}}/g \\ &= -NJ\mathbb{1} - J\sum_{j=1}^{N}\hat{P}_{j,j+1} + 2J\sum_{j=1}^{N}|s\rangle \\ &\quad\times\langle s|\hat{P}_{j,j+1}|s\rangle\langle s|,\end{aligned} \tag{B4}$$

where $|s\rangle\langle s|$ is the projector on the snippet basis, so that the last term applies only on diagonal elements. From this writing, it is clear the origin of the SB: the term $-J\sum_{j=1}^{N}\hat{P}_{j,j+1}$ is the bosonic one, while the term $+2J\sum_{j=1}^{N}|s\rangle\langle s|\hat{P}_{j,j+1}|s\rangle\langle s|$ is at the origin of a partial fermionization acting only partially on the system (on the diagonal terms). One can show that

$$2J\sum_{j=1}^{N}|s\rangle\langle s|\hat{P}_{j,j+1}|s\rangle\langle s| = J\sum_{j=1}^{N}\left(\mathbb{1} + 4S_z^{(j)}S_z^{(j+1)}\right). \tag{B5}$$

Thus, we get a XXZ Heisenberg chain Hamiltonian:

$$\begin{aligned}-\frac{V^{\mathrm{SB}}}{g} &= -2J\sum_{j=1}^{N}\left(S_x^{(j)}S_x^{(j+1)} + S_y^{(j)}S_y^{(j+1)} - S_z^{(j)}S_z^{(j+1)}\right) \\ &\quad - \tfrac{1}{2}NJ\mathbb{1}.\end{aligned} \tag{B6}$$

Remark that such a XXZ Hamiltonian can me mapped on a XXX one with an opposite sign of J by applying the unitary transformation $U = \prod_{\ell=even} 2S_z^{(\ell)}$ [21,34]. Such an operator *does not preserve the symmetry* (does not commute with the operator $\Gamma^{(2)}$), and its action is equivalent to mapping TG

bosons on noninteracting fermions and vice versa. On our snippet basis,

$$U = \begin{pmatrix} -1 & 0 & 0 & 0 & 0 & 0 \\ 0 & 1 & 0 & 0 & 0 & 0 \\ 0 & 0 & -1 & 0 & 0 & 0 \\ 0 & 0 & 0 & -1 & 0 & 0 \\ 0 & 0 & 0 & 0 & 1 & 0 \\ 0 & 0 & 0 & 0 & 0 & -1 \end{pmatrix}. \tag{B7}$$

APPENDIX C: THE MATRIX $\Gamma^{(2)}$

For the case of a balanced mixture of $N = 4$ bosons, the $\Gamma^{(2)}$ matrix can be written in the snippet basis [taking into account the initial ansatz for the many-body wave function (2)] as

$$\Gamma^{(2)} = \begin{pmatrix} 2 & 1 & 1 & 1 & 1 & 0 \\ 1 & 2 & 1 & 1 & 0 & 1 \\ 1 & 1 & 2 & 0 & 1 & 1 \\ 1 & 1 & 0 & 2 & 1 & 1 \\ 1 & 0 & 1 & 1 & 2 & 1 \\ 0 & 1 & 1 & 1 & 1 & 2 \end{pmatrix}, \tag{C1}$$

which can be diagonalized. This yields three representations of dimension 1, 3, and 2 with eigenvalues $\gamma_2 = 6, 2, 0$ corresponding to the diagrams $\square\square\square\square$, $\begin{smallmatrix}\square\square\\\square\square\end{smallmatrix}$, and $\begin{smallmatrix}\square\square\\\square\square\end{smallmatrix}$. The eigenstate corresponding the irreductible representation of dimension one is $\vec{v}_6 = \frac{1}{\sqrt{6}}(1, 1, 1, 1, 1, 1)$, which is identical to the ground state of the SU(2) model. The other eigenvectors are $\vec{v}_{2_1} = \frac{1}{\sqrt{2}}(-1, 0, 0, 0, 0, 1)$, $\vec{v}_{2_2} = \frac{1}{\sqrt{2}}(0, -1, 0, 0, 1, 0)$, $\vec{v}_{2_3} = \frac{1}{\sqrt{2}}(0, 0, -1, 1, 0, 0)$, $\vec{v}_{0_1} = \frac{1}{2}(1, 0, -1, -1, 0, 1)$, and $\vec{v}_{0_2} = \frac{1}{2\sqrt{3}}(1, -2, 1, 1, -2, 1)$. The ground state of the system with broken SU(2) symmetry will be a linear superposition of states with different symmetries. In this precise case we obtain that $\vec{a}_P^{\,\mathrm{SB}} = \frac{2\sqrt{2}}{3}\vec{v}_6 + \frac{1}{3}\vec{v}_{0_2}$, namely, the symmetries involved are mainly $\square\square\square\square$ $(\frac{8}{9})$ but also $\begin{smallmatrix}\square\square\\\square\square\end{smallmatrix}$ $(\frac{1}{9})$.

APPENDIX D: LINK BETWEEN $\Gamma^{(2)}$ AND $\vec{S}^2$

The objective of this Appendix is to build a bridge between the symmetry framework (two-cycle class-sum operator) and the more usual formalism of spin matrices. In this perspective we first express the swapping operator for $\kappa = 2$ mixtures in term of $\vec{S}^{(n)} = (S_x^{(n)}, S_y^{(n)}, S_z^{(n)})$. This one reads

$$\hat{P}_{i,j} = 2\vec{S}^{(i)} \cdot \vec{S}^{(j)} + \tfrac{1}{2}\mathbb{1}. \tag{D1}$$

Then we remark that

$$\Gamma^{(2)} = \sum_{i<j} \hat{P}_{i,j} = 2\sum_{i<j} \vec{S}^{(i)} \cdot \vec{S}^{(j)} + \frac{N(N-1)}{4}\mathbb{1} \tag{D2}$$

and

$$\begin{aligned} |\vec{S}^2| &= \sum_{i,j} \vec{S}^{(i)} \cdot \vec{S}^{(j)} \\ &= \sum_{i<j} \vec{S}^{(i)} \cdot \vec{S}^{(j)} + \sum_{j<i} \vec{S}^{(i)} \cdot \vec{S}^{(j)} + \sum_i |\vec{S}^{(i)}|^2 \\ &= 2\sum_{i<j} \vec{S}^{(i)} \cdot \vec{S}^{(j)} + \sum_i |\vec{S}^{(i)}|^2, \end{aligned} \tag{D3}$$

which lead for $\Gamma^{(2)}$:

$$\Gamma^{(2)} = |\vec{S}|^2 - \sum_i |\vec{S}^{(i)}|^2 + \frac{N(N-1)}{4}\mathbb{1}. \tag{D4}$$

Taking into account that $|\vec{S}^{(i)}|^2 = \frac{3}{4}\mathbb{1}$, $\forall i$, we end up with a straightforward relation between $\Gamma^{(2)}$ and $\vec{S}^2$:

$$\Gamma^{(2)} = |\vec{S}|^2 + \frac{N(N-4)}{4}\mathbb{1}. \tag{D5}$$

APPENDIX E: DEMONSTRATION OF THE SU(κ) SYMMETRY BREAKING

For the case of $N = 4$ one can easily calculate the commutators $[V^{\mathrm{SU}}, \Gamma^{(2)}]$ and $[V^{\mathrm{SB}}, \Gamma^{(2)}]$ using the explicit form of the matrices (A1), (A2), and (C1). The first is zero, legitimating the use of the Young tableaux for the identification of the symmetries of the eigenstates, while the second is different from zero, which is a proof of SB.

In this Appendix we generalize our demonstration to the case of arbitrary N particles, for a homogeneous system or in the case of an inhomogeneous trapping potential (including a site dependence on the exchange J terms, $J \to J_j$), and extending the discussion to any $SU(\kappa)$ mixture. Indeed, the introduction of other spin components affects only the definition of the snippet basis.

Let us start by writing the matrices $\Gamma^{(2)}$ and V^{SU} as a function of the permutation operators. Using the (B1) form of V^{SU}/g, we see that the commutator $[V^{\mathrm{SU}}, \Gamma^{(2)}]$ reduced to $\sim[\sum_i J_i \hat{P}_{i,i+1}, \sum_{i'<j'} \hat{P}_{i',j'}] = \frac{1}{2}[\sum_i J_i \hat{P}_{i,i+1}, \sum_{i',j'} \hat{P}_{i',j'}]$. Then one can write the permutations operators in the second quantization framework as following [35]

$$\hat{P}_{i,j} = \sum_{\mu,\nu} F_\mu^\nu(i) F_\nu^\mu(j), \tag{E1}$$

where $F_\mu^\nu(i) = a_{i,\mu}^\dagger a_{i,\nu}$, a and $a^\dagger$ are usual annihilation and creation operators (fermionic or bosonic), μ and ν are the spin-s projection indices going from 1 to $2s+1$, and i and j are the sites indices. It is important to notice that the $F_\mu^\nu(i)$ are the generators of the SU(κ) group, satisfying the commutation relation of the SU(κ) Lie algebra

$$\left[F_\mu^\nu(i), F_{\nu'}^{\mu'}(j)\right] = \delta_i^j\left[\delta_{\mu'}^\nu F_{\mu'}^{\nu'}(i) - \delta_\mu^{\nu'} F_{\mu'}^\nu(j)\right]. \tag{E2}$$

By using the commutation relation (E2), one find that $[\sum_i J_i P_{i,j}, \sum_{i',j'} P_{i',j'}] = 0$ for any j, and thus also for $j = i+1$. Starting with the (B4) form of V^{SB} one can find that $[V^{\mathrm{SB}}/g, \Gamma^{(2)}] = [4\sum_j J_j S_z^{(j)} S_z^{(j+1)}, 2\sum_{n,j'} \vec{S}^{(j')}\vec{S}^{(j'+n)}]$. Again, using the commutation relation of spin matrices, it is straightforward to obtain that

$$\begin{aligned} [V^{\mathrm{SB}}/g, \Gamma^{(2)}] = \; & 8\sum_{j,n} J_j\big[\big(S_+^{(j)}S_-^{(j+n)} - S_-^{(j)}S_+^{(j+n)}\big) \\ & \times \big(S_z^{(j+n+1)} - S_z^{(j+1)}\big) + \big(S_z^{(j+n-1)} - S_z^{(j-1)}\big) \\ & \times \big(S_+^{(j)}S_-^{(j+n)} - S_-^{(j)}S_+^{(j+n)}\big)\big], \end{aligned} \tag{E3}$$

which does not vanish regardless the type of mixture ($\forall\kappa$) and/or the number of particles ($N > 2$).

APPENDIX F: DEMONSTRATION OF EQ. (27)

Let us consider the Hamiltonian (1)

$$\hat{H} = H_{\rm kin} + \sum_{\sigma=\uparrow,\downarrow} \hat{H}_{{\rm int},\sigma\sigma} + H_{{\rm int},\uparrow\downarrow}, \tag{F1}$$

where we have defined $H_{kin} = \sum_{\sigma=\uparrow,\downarrow} \sum_i^{N_\sigma} -\frac{\hbar^2}{2m}\frac{\partial^2}{\partial x_{i,\sigma}^2}$, $H_{{\rm int},\sigma\sigma} = g_{\sigma\sigma} \sum_i^{N_\sigma} \sum_{j>i}^{N_\sigma} \delta(x_{i,\sigma} - x_{j,\sigma})$, and $H_{int,\uparrow\downarrow} = g_{\uparrow\downarrow} \sum_i^{N_\uparrow} \sum_j^{N_\downarrow} \delta(x_{i,\uparrow} - x_{j,\downarrow})$.

The first step is to make the Fourier transform of the Schrödinger equation $\hat{H}\Psi = E\Psi$ with respect, for instance, to x_1. Let σ be the spin of such a particle. In the large-momentum limit, using that $\lim_{k\to\infty} \Psi(k, x_2, \ldots, x_N) = 0$, one gets

$$\lim_{k\to\infty} \frac{\hbar^2 k^2}{2m} \Psi(k, x_2, \ldots, x_N) = g_{\uparrow\downarrow} \sum_{j,\sigma'\neq\sigma} \Psi(x_{j,\sigma'}, \ldots, x_{j,\sigma'}, \ldots) e^{-ikx_{j,\sigma'}} + \sum_{\sigma=\uparrow,\downarrow} g_{\sigma\sigma} \sum_{j,\sigma} \Psi(x_{j,\sigma}, \ldots, x_{j,\sigma}, \ldots) e^{-ikx_{j,\sigma}}. \tag{F2}$$

By multiplying by the complex conjugate, one obtains the following asymptotic behavior of the total momentum distribution $n(k)$:

$$\lim_{k\to\infty} k^4 n(k) = \frac{2m^2}{\hbar^4} \left(g_{\uparrow\downarrow} \langle \Psi | \hat{H}_{{\rm int},\uparrow\downarrow} | \Psi \rangle + \sum_{\sigma=\uparrow,\downarrow} g_{\sigma\sigma} \langle \Psi | \hat{H}_{{\rm int},\sigma\sigma} | \Psi \rangle \right). \tag{F3}$$

By applying the Hellmann-Feynman theorem, it is straightforward to show that Eq. (F3), with Ψ the symmetry-breaking many-body wave function, gives Eq. (27) in the Tonks-Girardeau limit.

[1] V. Yurovsky, M. Olshanii, and D. Weiss, Adv. Atomic Mol. Optical Phys. **55**, 61 (2008).
[2] M. A. Cazalilla, R. Citro, T. Giamarchi, E. Orignac, and M. Rigol, Rev. Mod. Phys. **83**, 1405 (2011).
[3] X.-W. Guan, M. T. Batchelor, and C. Lee, Rev. Mod. Phys. **85**, 1633 (2013).
[4] T. Sowiński and M. Á. García-March, Rep. Prog. Phys. **82**, 104401 (2019).
[5] A. Minguzzi and P. Vignolo, AVS Quantum Sci. **4**, 027102 (2022).
[6] S. Mistakidis, A. Volosniev, R. Barfknecht, T. Fogarty, T. Busch, A. Foerster, P. Schmelcher, and N. Zinner, arXiv:2202.11071 (2022).
[7] M. Girardeau, Phys. Rev. **139**, B500 (1965).
[8] E. H. Lieb, Phys. Rev. **130**, 1616 (1963).
[9] C. N. Yang, Phys. Rev. Lett. **19**, 1312 (1967).
[10] B. Sutherland, Phys. Rev. Lett. **20**, 98 (1968).
[11] J. B. McGuire, J. Math. Phys. **5**, 622 (1964).
[12] P. Calabrese and J.-S. Caux, Phys. Rev. Lett. **98**, 150403 (2007).
[13] L. Piroli and P. Calabrese, Phys. Rev. A **94**, 053620 (2016).
[14] M. Gaudin, Phys. Lett. A **24**, 55 (1967).
[15] X.-W. Guan and T.-L. Ho, Phys. Rev. A **84**, 023616 (2011).
[16] F. Deuretzbacher, K. Fredenhagen, D. Becker, K. Bongs, K. Sengstock, and D. Pfannkuche, Phys. Rev. Lett. **100**, 160405 (2008).
[17] J. Decamp, P. Armagnat, B. Fang, M. Albert, A. Minguzzi, and P. Vignolo, New J. Phys. **18**, 055011 (2016).
[18] J. Decamp, J. Jünemann, M. Albert, M. Rizzi, A. Minguzzi, and P. Vignolo, Phys. Rev. A **94**, 053614 (2016).
[19] J. Decamp, J. Juenemann, M. Albert, M. Rizzi, A. Minguzzi, and P. Vignolo, New J. Phys. **19**, 125001 (2017).
[20] F. Deuretzbacher, D. Becker, J. Bjerlin, S. M. Reimann, and L. Santos, Phys. Rev. A **90**, 013611 (2014).
[21] A. G. Volosniev, D. Petrosyan, M. Valiente, D. V. Fedorov, A. S. Jensen, and N. T. Zinner, Phys. Rev. A **91**, 023620 (2015).
[22] F. Deuretzbacher, D. Becker, and L. Santos, Phys. Rev. A **94**, 023606 (2016).
[23] G. Pecci, P. Vignolo, and A. Minguzzi, Phys. Rev. A **105**, L051303 (2022).
[24] M. Rizzi, C. Miniatura, A. Minguzzi, and P. Vignolo, Phys. Rev. A **98**, 043607 (2018).
[25] F. T. Sant'Ana, F. Hébert, V. G. Rousseau, M. Albert, and P. Vignolo, Phys. Rev. A **100**, 063608 (2019).
[26] P. Capuzzi and P. Vignolo, Phys. Rev. A **101**, 013633 (2020).
[27] E. Lieb and D. Mattis, Phys. Rev. **125**, 164 (1962).
[28] A. G. Volosniev, D. V. Fedorov, A. S. Jensen, N. T. Zinner, and M. Valiente, Nat. Commun. **5**, 5300 (2014).
[29] R. E. Barfknecht, A. Foerster, N. T. Zinner, and A. G. Volosniev, Commun. Phys. **4**, 252 (2021).
[30] G. James and A. Kerber, *The Representation Theory of the Symmetric Group* (Addison-Wesley, Reading, MA, 1981).
[31] G. James and M. Liebeck, *Representations and Characters of Groups*, 2nd ed. (Cambridge University Press, Cambridge, 2001).
[32] P. J. Forrester, N. E. Frankel, T. M. Garoni, and N. S. Witte, Phys. Rev. A **67**, 043607 (2003).
[33] S. Tan, Ann. Phys. **323**, 2971 (2008).
[34] M. Takahashi, in *Thermodynamics of One-Dimensional Solvable Models* (Cambridge University Press, Cambridge, 1999).
[35] A. Auerbach, *Interacting Electrons and Quantum Magnetism* (Springer, New York, 1994).

Correction: Minor errors in Eqs. (16) and (17) have been fixed. Corresponding changes to the surrounding text have also been made.

Second Correction: The Young tableaux in the text following Eqs. (12) and (C1) were presented incorrectly as a result of a processing error in production and have been fixed.